Radiation Induced Absorption in Rare Earth Doped Optical Fibers

M. Lezius, K. Predehl, W. Stöwer, A. Türler, M. Greiter, Ch. Hoeschen, P. Thirolf, W. Assmann, D. Habs, A. Prokofiev, C. Ekström, T. W. Hänsch, and R. Holzwarth

***Abstract*—We have investigated the radiation induced absorption (RIA) of optical fibers with high active ion concentration. Comparing our results to the literature leads us to the conclusion that RIA appears to be only weakly dependent on the rare earth dopant concentration. Instead, co-dopants like Al, Ge, or P and manufacturing processes seem to play the major role for the radiation sensitivity. It is also observed that different types of irradiation cause very similar RIA at the same dose applied, with the exception at very high dose rates. It has been studied how RIA can be efficiently reduced via moderate heating. Recovery of up to 70% of the original transmission has been reached after annealing at 450 K. We conclude that radiation induced color centers have weak binding energies between 20 and 40 meV. This suggests that annealing could become a key strategy for an improved survival of rare earth doped fibers in radiative environments, opening up new possibilities for long-term missions in space.**

***Index Terms*—Color centers, erbium, gamma, neutrons, optical fibers, protons, radiation effects, ytterbium.**

I. Introduction

RARE earth doped optical fibers represent a key element in modern laser technology. The core of such fibers can be doped with substantial amounts of the trivalent ions of Yb, Y, Nd, Er, Ce, Ho, and their mixtures, which provides an interesting gain medium in which light is guided by the fiber [1]. The efficiency and robustness of lasers based on such fibers have been fundamental for their success. It has been demonstrated that fiber lasers in combination with fiber amplifiers can be powerful light sources, providing optical power beyond 800 W [2]. Moreover, mode-locked fiber laser oscillators can be engineered for sufficient bandwidth to support femtosecond pulses [3] and, using appropriate spectral splitting and amplification, even few-cycle pulses (4.3 fs) have been reported [4]. It has also been demonstrated that femtosecond fiber lasers can be phase stabilized to provide frequency combs [5]. Robustness, size, weight, and efficiency also make fiber lasers a preferential choice for applications in radiation environments such as space.

The Earth's magnetic field efficiently traps energetic electrons and ions into radiation belts, also known as Van Allen belts. In the radiation belts electron energies of up to a few MeV energy and protons of up to several hundred MeV energy are present [6]. The abundance of such particles varies strongly, e.g., in the so-called South Atlantic Anomaly dose rates reaching 200 mSv/h behind 3 mm aluminum can be orders of magnitude higher compared to typical Van Allen belt irradiations of $\sim$1 mSv/d. Moreover, the Sun emits energetic particles not constantly, but rather with a cyclic intensity having a typical period of 10.7 years. Therefore careful documentation of the radiation hardness of each part involved is an important prerequisite for successful space applications. Many parts like bulk optics and typical electronics found in fiber comb lasers have already been space qualified and can be looked up in NEPP [7] or at ESCIES [8]. Heuristically one can state that such optical parts consisting mainly from SiO_2 can be considered to be sufficiently hard to radiation if 90% performance is preserved after receiving a dose of 1 kGy into the respective material. Regarding irradiation of optical fibers, a substantial number of doped and undoped fibers have been reported in [9]. However, less information is available regarding the radiation hardness of rare earth doped fibers with high dopant concentrations. Moreover, present studies on the radiation hardness of various commercial fibers exhibit only little systematic trends. With the present work, we aim to shed more light on this knowledge gap, to evaluate the radiation hardness of highly doped fibers and to suggest strategies that promise to extend fiber lifetimes substantially.

A. Previous Investigations on Rare Earth Doped Fibers

The radiation hardness of rare earth doped fibers has been investigated since 1978 [10]–[13], often having space applications in mind [14]. Comparative studies on various such fibers under gamma irradiation have been performed [14]–[22]. It has been reported that for fibers doped with rare earth atoms the radiation sensitivity is often increased by orders of magnitude (with typical values between 0.001 and 0.1 $\mathrm{dBGy^{-1}m^{-1}}$) compared to typical single mode communication fibers like the SMF28 by Dow Corning ($\sim$0.0005 $\mathrm{dBGy^{-1}m^{-1}}$). RIA of rare earth doped fibers has been interpreted in the context of color center

Manuscript received July 05, 2011; revised August 12, 2011; accepted September 06, 2011. Date of publication February 07, 2012; date of current version April 13, 2012. This work was supported in part by the DLR micro gravity programme (coordinated by R. Kuhl) within the project FOKUS.

M. Lezius is with Menlo Systems GmbH, 82152 Martinsried, Germany.

R. Holzwarth is with Menlo Systems GmbH, 82152 Martinsried, Germany, and also with the Max-Planck-Institute for Quantum Optics, 85748 Garching, Germany (e-mail: r.holzwarth@menlosystems.com).

K. Predehl and T. W. Hänsch are with the Max-Planck-Institute for Quantum Optics, 85748 Garching, Germany.

W. Stöwer is with the Institute for Radiochemistry, Technical University Munich, 85748 Garching, Germany.

A. Türler is with the Paul Scherrer Institute, Laboratory for Radiochemistry and Environmental Chemistry, CH5232 Villigen, Switzerland.

M. Greiter and Ch. Hoeschen are with the Helmholtz Center Munich, 85764 Neuherberg, Germany.

P. Thirolf, W. Assmann, and D. Habs are with the Department of Physics, Ludwig-Maximilans University Munich, Garching 85748, Germany.

A. Prokofiev and C. Ekström are with The Svedberg Laboratory, S-75121 Uppsala, Sweden.

Color versions of one or more of the figures in this paper are available online at http://ieeexplore.ieee.org.

Digital Object Identifier 10.1109/TNS.2011.2178862

generation, facilitated by atoms or clusters of the dopant. RIA has been reported to be in a first order independent on the type of ionizing radiation, in particular when comparing protons, gamma, and x-rays [14], [18]. Also, in the low dose limit, the dose rate appears to play a rather minor role [17]. Fibers have been found to be sensitive to neutron irradiation [23], but at the same dose rates degradation has been found to be significantly slower, about half as fast compared to gamma irradiation. Moreover, at least in the case of Er, the rare earth dopant concentration itself does not seem to strongly or non-linearly influence RIA [20]. In some cases it appears to be the amount of co-dopants, in particular of Al, which increases the fiber radiation sensitivity [18]. Aluminum is often added to the glass to increase the solubility of dopants and to prevent clustering, especially at high dopant concentrations. Typical fibers used in femtosecond fiber lasers are highly doped, because the dispersion management and the repetition rate of such lasers asks for comparably short fiber loops. High dopant concentrations of Al often goes along with an increased Ge doping. Within this work we have recompiled a substantial number of studies on rare earth doped fibers [14]–[22]. In particular, we have been searching for correlations of RIA with various experimental and fiber parameters. To evaluate the radiation hardness the radiation induced absorption A was modeled using the *Power Law* [13]

$$A(D) = \alpha \cdot D^{\beta} \tag{1}$$

where D is the dose and α and β are fiber-dependent parameters. $A(t) = I(t)/I(0)$ of the transmitted light I is usually given here in dB. The Power Law has been found to model RIA for many fibers reasonably well, especially for extended irradiation at low dose rates. From our comparison we find that the exponent β is mostly in the range between 0.7 and 1.0. However, the prefactor α dominates the RIA and varies strongly and non-systematically over several orders of magnitude. This is shown in Fig. 1, which plots α versus dopant concentration. For erbium general trend appears to be that $\alpha = C^{1.37}$. However, for a fixed dopant concentration C the coefficient α can be seen to vary over three orders of magnitude. Table I summarizes our literature research, including data from our own experiments (marked t.w. for 'this work'). The table is sorted by increasing radiation sensitivity α. From our comparison we conclude that the prediction of radiation sensitivity for a given fiber appears to be rather difficult. Instead the RIA for a given fiber should be directly derived from irradiation experiments.

Radiation induced color centers (CC) are created by carriers that become trapped near matrix defects. In general, they are unstable and decay (multi-)exponentially, however, at room temperature they decay quite slowly. CCs are well known and have been thoroughly investigated in bulk glass material. Their absorption can in many cases be partially or even totally reversed via thermal annealing or bleaching. In Ge-doped fibers, for example, bleaching was found to be more efficient with 900 nm light than with UV [24]. Moreover, RIA has been significantly reduced when the fiber is heated during the irradiation process [25], [26]. In a prototypical fiber amplifier irradiation experiment it was found that RIA is much less severe in an actively pumped Yb fiber than in a passively irradiated one [27]. Comparing Yb and Er it has also been documented that Er-doped fibers are more sensitive to irradiation [17]. This study also compared the annealing behavior of a large set of fibers. The concentration of the co-dopants Al and Ge appears to be responsible for an increased radiation sensitivity [28]. However, co-dopants can also improve the radiation hardness. For example, high pressure treatment with hydrogen has been reported to increase radiation hardness by about a factor 5 [29]–[31]. Similarly, Ce can be added to the glass to increase its radiation hardness [32], [33]. It has been reported recently that Yb doped fiber amplifiers exhibit less photo-darkening effects, if small amounts of Ce are added to the core [34]. In sum, rare earth doped fibers have been found to be quite sensitive to ionizing irradiation with substantial RIA but, on the other hand, some strategies exist to increase the radiation hardness towards levels necessary for space missions.

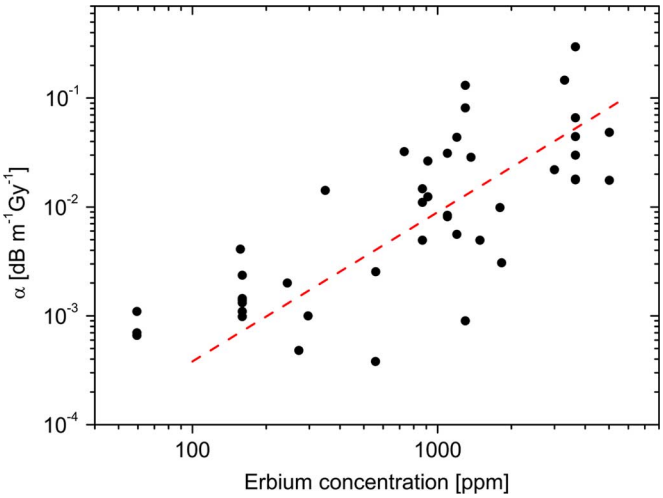

Fig. 1. Preexponential factor α of the Power Law (1) plotted against the dopant concentration C. These values have been extracted from the literature data for erbium-doped fibers summarized in Table I. The dotted line corresponds to an exponential dependence like $\alpha \propto C^{1.37}$.

II. Experimental

We have irradiated several fibers that are prototypical to fiber lasers with highly energetic ionizing particles that are present in near-Earth and solar systems' space: Protons at selected energies, neutrons, and gamma rays. Electrons have been omitted in this study, because their penetration depth is usually low and they can be efficiently shielded. All irradiated fibers are commercially available core doped single clad fibers with a core diameter between 4 and 9 μm, a cladding diameter of 125 μm, and a coating diameter of 250 μm.

For quantitative measurement of the fiber transmission, the fiber was coupled to a 1310 nm telecommunication laser (DFB-1310-BF-10-2.5-FA, Applied Optoelectronics). This laser was operated current and temperature stabilized using a Pro800 and an ITC8102 laser supply (Thorlabs). The laser temperature was optimized to 26.1°C, where the laser shows an emission maximum. In the case of gamma irradiation, the laser light was split with a 1×4 splitter (SSWC-M-1550-250S-1X4-25-3-N, Photop), which enabled us to compare three different fibers simultaneously. The doped fiber length was between 800 mm and

TABLE I
RIA OF DOPED FIBERS SORTED BY INCREASING VALUE OF α. FIBERS INVESTIGATED IN THIS WORK ARE MARKED WITH T.W.('THIS WORK'), OTHERWISE REFERENCES ARE GIVEN. THE COEFFICIENTS α AND β HAVE BEEN EITHER PROVIDED BY THE REFERENCE, OR THE REFERENCE DATA HAS BEEN FIT HERE TO THE POWER LAW. THE RADIATION COLUMN MARKS THE TYPE OF RADIATION AND/OR THE ENERGY IN MEV

Nr	Name	Vendor	Dopant	C[ppm]	Al[%m]	Ge[%m]	P[%m]	Radiation	Flux[Gy/s]	α[dB/m/Gy]	β	Auth.
1	Er80-4/125	Liekki	Er	3657,14	n.s.	n.s.	n.s.	P- 2.6	6,96E+4	3,52E-5	7,90E-1	t.w.
2	SMF28	Corning	none	0	0,0	3,0	0,0	G Co	2,00E-2	2,17E-4	5,92E-1	t.w.
3	HG 980	OFS	Er	558,23	10,0	22,0	0,0	G Co	1,40E-1	3,80E-4	1,00E+0	[22]
4	SMF28	Corning	none	0	0,0	3,0	0,0	G Co	2,00E-2	4,78E-4	6,69E-1	[15]
5	LP 980	Lucent	Er	272,14	6,0	20,0	0,0	G Co	1,40E-1	4,80E-4	1,00E+0	[22]
6	n.s.	unknown	Er	59,43	n.s.	n.s.	n.s.	G Co	7,47E-2	6,62E-4	8,36E-1	[16]
7	n.s.	unknown	Er	59,43	n.s.	n.s.	n.s.	G Co	8,89E-3	6,99E-4	7,65E-1	[16]
8	n.s.	unknown	Er	59,43	n.s.	n.s.	n.s.	G Co	7,47E-2	6,99E-4	7,65E-1	[16]
9	31s	IPHT	Ho	1300	1,0	5,0	1,2	G Co	3,00E-2	9,00E-4	9,50E-1	[17]
10	33s	IPHT	Yb	10000	1,0	5,0	1,2	G Co	3,00E-2	9,00E-4	8,80E-1	[17]
11	HE 980	OFS	Er	160	16,0	28,0	0,0	P 63	8,33E-3	9,85E-4	8,04E-1	[14]
12	MP 980	OFS	Er	296,56	n.s.	n.s.	n.s.	G Co	1,40E-1	1,00E-3	1,00E+0	[22]
13	HE 980	OFS	Er	160	12,0	20,0	0,0	G Co	8,33E-3	1,10E-3	7,90E-1	[14]
14	n.s.	unknown	Er	59,43	n.s.	n.s.	n.s.	G Co	8,89E-3	1,10E-3	6,45E-1	[16]
15	HE 980	OFS	Er	160	12,0	20,0	0,0	P 63	1,83E-1	1,32E-3	7,97E-1	[14]
16	HE 980	OFS	Er	160	12,0	20,0	0,0	G Co	1,81E-1	1,39E-3	7,99E-1	[14]
17	HE 980	OFS	Er	160	12,0	20,0	0,0	G Co	1,83E-1	1,39E-3	7,93E-1	[14]
18	HE 980	OFS	Er	160	12,0	20,0	0,0	P 63	1,83E-1	1,42E-3	7,92E-1	[14]
19	HE 980	OFS	Er	160	12,0	20,0	0,0	G Co	1,83E-1	1,44E-3	7,92E-1	[14]
20	HP 980	OFS	Er	244,23	6,0	0,0	0,0	G Co	1,40E-1	2,00E-3	1,00E+0	[22]
21	HE 980	OFS	Er	160	12,0	20,0	0,0	G Co	3,33	2,36E-3	7,80E-1	[14]
22	HG 980	OFS	Er	560	10,0	22,0	0,0	P 63	1,83E-1	2,55E-3	7,02E-1	[14]
23	ErYb PM 125	OFS	Er/Yb	1828,57	n.s.	n.s.	n.s.	G Co	4,10E-1	3,08E-3	9,35E-1	[19]
24	HE 980	OFS	Er	157	12,0	20,0	16,0	G Co	1,40E-1	4,10E-3	1,00E+0	[22]
25	SM-EYDF	Nufern	Er/Yb	1490,29	n.s.	n.s.	n.s.	G Co	1,96E-1	4,94E-3	1,00E+0	[15]
26	SM-EYSF	Nufern	Er/Yb	868,57	n.s.	n.s.	n.s.	G Co	1,96E-1	4,94E-3	1,00E+0	[15]
27	45s	IPHT	Nd	8000	4,5	0,0	0,5	G Co	3,00E-2	5,00E-3	9,50E-1	[17]
28	29s	IPHT	Nd	1200	1,0	6,7	0,9	G Co	3,00E-2	5,60E-3	9,60E-1	[17]
29	Yb1200-4/125	Liekki	Yb	9780	n.s.	n.s.	n.s.	G Co	4,10E-1	6,73E-3	9,06E-1	t.w.
30	89s	IPHT	Yb	1800	4,2	0,0	0,9	G Co	3,00E-2	9,90E-3	9,90E-1	[17]
31	Yb1200-20/400 DC	Liekki	Yb	9780	n.s.	n.s.	n.s.	G Co	4,10E-1	1,08E-2	9,06E-1	[19]
32	Yb1200-4/125	Liekki	Yb	9780	n.s.	n.s.	n.s.	G Co	4,10E-1	1,12E-2	9,31E-1	[19]
33	Er30-4/125	Liekki	Er	914,29	n.s.	n.s.	n.s.	G Co	1,00E-2	1,24E-2	9,28E-1	t.w.
34	R37003	OFS	Er	348,9	n.s.	n.s.	n.s.	P, G Co	1,40E-1	1,42E-2	1,00E+0	[22]
35	Yb1200-4/125DC	Liekki	Yb	9780	n.s.	n.s.	n.s.	G Co	1,40E-1	1,49E-2	9,63E-1	[19]
36	Yb2000-6/125DC	Liekki	Yb	16300	n.s.	n.s.	n.s.	G Co	4,10E-1	1,59E-2	8,79E-1	[19]
37	Yb1200-4/125	Liekki	Yb	9780	n.s.	n.s.	n.s.	G Co	4,10E-1	1,73E-2	9,40E-1	[19]
38	Yb1200-30/250DC	Liekki	Yb	9780	n.s.	n.s.	n.s.	G Co	4,10E-1	1,76E-2	9,05E-1	[19]
39	Er110-4/125	Liekki	Er	5028,57	n.s.	n.s.	n.s.	G Co	1,00E-2	1,76E-2	9,32E-1	t.w.
40	Yb2000-6/125DC	Liekki	Yb	16300	n.s.	n.s.	n.s.	G Co	1,40E-1	1,78E-2	9,45E-1	[21]
41	Er80-4/125	Liekki	Er	3657,14	n.s.	n.s.	n.s.	G Co	1,00E-2	1,78E-2	9,32E-1	t.w.
42	Er80-4/125	Liekki	Er	3657,14	n.s.	n.s.	n.s.	G Co	4,10E-1	1,80E-2	9,20E-1	t.w.
43	Yb1200-20/40DC	Liekki	Yb	9780	n.s.	n.s.	n.s.	G Co	4,10E-1	1,91E-2	8,84E-1	[19]
44	Er80-4/125	Liekki	Er	3657,14	n.s.	n.s.	n.s.	P- 20	1,24E+2	2,00E-2	9,0E-1	t.w.
45	95s	IPHT	Ho	3000	6,0	0,0	0,4	G Co	3,00E-2	2,20E-2	9,80E-1	[17]
46	Er80-4/125	Liekki	Er	3657,14	n.s.	n.s.	n.s.	P- 180	7,1E-0	2,2E-2	9,07E-1	t.w.
47	Yb1200-30/250DC	Liekki	Yb	9780	n.s.	n.s.	n.s.	G Co	4,10E-1	2,33E-2	8,62E-1	[19]
48	Yb2000-6/125DC	Liekki	Yb	16300	n.s.	n.s.	n.s.	G Co	4,10E-1	2,40E-2	8,98E-1	[19]
49	Er20-4/125	Liekki	Er	914,29	n.s.	n.s.	n.s.	G Co	4,10E-1	2,65E-2	9,37E-1	[19]
50	Er30-4/125	Liekki	Er	1371,43	n.s.	n.s.	n.s.	G Co	4,10E-1	2,86E-2	9,56E-1	[19]
51	Er80-4/125	Liekki	Er	3657,14	n.s.	n.s.	n.s.	G Co	2,12E-1	3,00E-2	1,24E+0	t.w.
52	EDFL-980-HP	Nufern	Er	1097,14	n.s.	n.s.	n.s.	P 55	3,30E-1	3,11E-2	8,27E-1	[40]
53	Er16-8/125	Liekki	Er	731,43	n.s.	n.s.	n.s.	G Co	4,10E-1	3,23E-2	9,26E-1	[19]
54	106s	IPHT	Gd	1200	3,5	0,0	1,0	G Co	3,00E-2	4,38E-2	9,40E-1	[17]
55	Er80-4/125	Liekki	Er	3657,14	n.s.	n.s.	n.s.	G Co	4,10E-1	4,43E-2	9,15E-1	[19]
56	960820-6-1-02-11	Lucent	La	18000	8,0	0,0	0,0	G Co	3,00E-2	4,70E-2	9,10E-1	[17]
57	Er110-4/125	Liekki	Er	5028,57	n.s.	n.s.	n.s.	G Co	4,10E-1	4,84E-2	9,35E-1	[19]
58	970514-06-1	Lucent	La	17000	5,0	0,0	0,0	G Co	3,00E-2	5,40E-2	9,20E-1	[17]
59	961107-6-2-04	Lucent	La/Er	18000	8,0	0,0	0,0	G Co	3,00E-2	5,47E-2	9,20E-1	[17]
60	970227-06-2	Lucent	La	20000	10,0	0,0	0,0	G Co	3,00E-2	6,33E-2	9,40E-1	[17]
61	970514-06-2	Lucent	La	20000	6,0	0,0	0,0	G Co	3,00E-2	6,74E-2	9,30E-1	[17]
62	970317-06-3	Lucent	La	20000	6,0	0,0	0,0	G Co	3,00E-2	8,50E-2	9,30E-1	[17]
63	960614-6-1-02	Lucent	La	18000	8,0	0,0	0,0	G Co	3,00E-2	8,83E-2	9,50E-1	[17]
64	112s	IPHT	Sm	1300	3,5	0,0	1,0	G Co	3,00E-2	1,31E-1	9,70E-1	[17]
65	94s	IPHT	Pr	3300	7,0	1,5	0,6	G Co	3,00E-2	1,46E-1	9,20E-1	[17]
66	90s	IPHT	Pr	1100	3,0	0,0	1,3	G Co	3,00E-2	3,38E-1	9,70E-1	[17]

1600 mm, depending on the experiment. Laser light was delivered to and from the irradiated section using SMF28 fibers (15 m long). Such fibers have been specified to be highly resistant to radiation damage. The test fibers were spooled on a plastic holder. Transmitted light was received by a standard fiber pigtailed photodiode (KPPD-2-900L-FC/APC, Photop) that was operated at 9 V bias. The resulting photocurrent was measured via the voltage drop on a 1 kΩ resistor, with typical values between 1 and 3 V. The signal was digitized with 14 bit resolution (accuracy 0.1 mV after averaging over 200 measurements) and

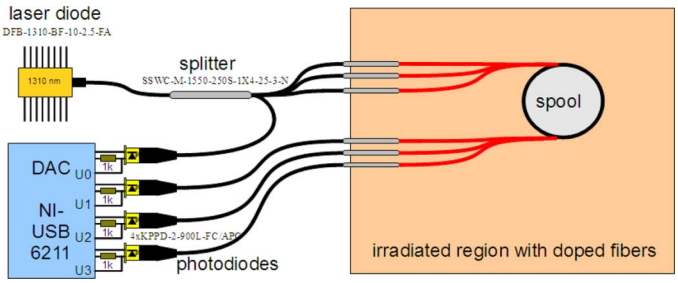

Fig. 2. Experimental set-up used for the comparison of RIA under Gamma irradiation.

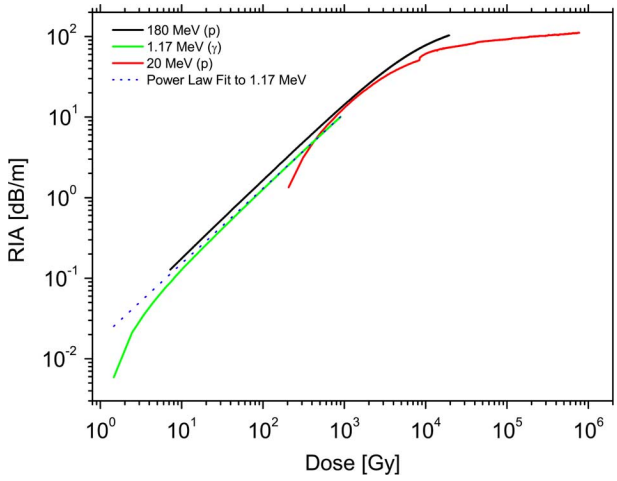

Fig. 3. RIA in the erbium-doped fiber Er80-4/125 (Liekki) after irradiation with protons of various energies and gamma-rays, measured at 1310 nm. Dotted line represents a fit according to (1) with $\alpha = 0.0178$ and $\beta = 0.93$ (see text).

logged by a computer at a rate of 1–2 Hz. The experimental set-up is shown in Fig. 2.

In the case of proton irradiation no splitter was used, which results in a larger error when comparing different fiber types. The length of the irradiated fiber varied between 10 mm and 200 mm, depending on the beam diameter. The fibers have been irradiated with protons of two selected energies: 20 MeV and 180 MeV. This deliberate selection of proton energies was based on our considerations that 20 MeV protons are representing typical space radiation with about 10^6 p/cm^{2}s while 180 MeV can not be shielded easily and their secondary effects appear to be difficult to predict. Protons of 20 MeV energy were produced in the Tandem accelerator of the LMU and TUM in Garching, Germany. Optical fibers were placed and irradiated in vacuum. The proton flux was calibrated for these measurements via the fluorescence from a CsI-crystal to be between $2.4 \ldots 5.0 \cdot 10^{10}$ p/cm^{2}s. Protons of 180 MeV were provided by the cyclotron accelerator at The Svedberg Laboratory, Sweden (TSL) [35] with a flux of $9 \cdot 10^9$ p/cm^{2}s. In addition a flux of $4 \cdot 10^7$ p/cm^{2}s was used in some experiments. At 180 MeV, protons are only weakly absorbed by most gases and therefore it was possible to perform these experiments in ambient air.

We have additionally irradiated some of the fibers with quasi-monoenergetic neutrons. Neutrons are obtained, when highly energetic protons are passing through a lithium target. These measurements were performed at the TSL [36] neutron facility with 20 MeV, and with 180 MeV neutrons. Flux densities for high-energy peak neutrons are about $0.3 \ldots 5 \cdot 10^5$ n/cm^{2}s. The observed fiber damage after several hours of exposure was very small.

Irradiation with gamma-rays is a convenient and established way to monitor radiation hardness of various components. Gamma radiation does not radio-activate the compound, which is desired for laboratory studies. Moreover, gamma sources are abundant in institutes and industry, and are easy to maintain. Therefore, quite a large number of studies exist on gamma irradiated fibers. Here, fibers have been irradiated with the characteristic gamma radiation of 1.17 and 1.33 MeV from a ^{60}Co source. Two sources have been used: a) at the Institute for Radiochemistry of the Technical University Munich, Germany (TUM) and b) at the Institute for Radiation Protection of the Helmholtz Center Munich, Germany. At a) higher dose rates of up to 0.48 Gy/s were applied, while at b) a much lower rate of 0.01 Gy/s was used. In a) the dose rate was estimated from the distance between source and target, in b) the dose rate in air (air kerma) was measured using a calibrated ionization chamber (PTW M 23331, 1 cm^3) coupled to a PTW UNIDOS electrometer. In b) ambient pressure was 962.2 mbar, and the temperature was 295.8 K. The evaluation of the data in a) shows that at such high dose rates non-linear effects come into play which prevents analysis according to (1).

Immediately after irradiation we studied the recovery of the fibers in situ and at room temperature. In addition, we have also initiated a separate annealing study with temperatures up to 450 K. The transmission has been logged via the photocurrent of a PD, when weak 1310 nm SM laser light is coupled into the fiber, identical to the transmission measurement shown in Fig. 2. For annealing, the fiber—apart from ca. 10 cm on each end including the splice—was placed in a laboratory oven which was slowly heated. Heating leads to a significant acceleration of the recovery and after about 24 h a transmission of up to 70% of the original value could be achieved.

After irradiation the fibers were inspected with various microscopic and spectroscopic techniques. With transmission electron microscopy (TEM) imaging, we were not able to detect any microscopic damage or changes of the amorphous structure of the fiber glass. Also, local X-ray fluorescence analysis (XRF) did not reveal any changes of the stoichiometry of the fiber in response to radiation. Inspection of the core reflectivity with an optical microscope showed only in one non-reproducible case some degradation. A comparative Raman analysis of the respective fiber core did not reveal any significant deviation from the unirradiated case.

III. Results

It is possible to compare quantitatively the RIA for different types of ionizing radiation. For Er80-4/125 produced by Liekki such a comparison is shown in Fig. 3, including the fit to the Power Law (1). It can immediately be seen that the Power Law can fit the data only in a certain range, but that the type of radiation plays a rather negligible role. In the beginning of the irradiation process the RIA generally rises stronger than (1) predicts. We observe that this tuning of the fiber into the Power Law

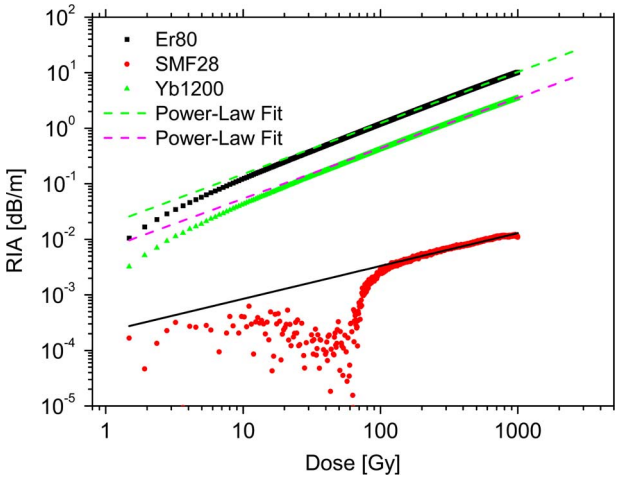

Fig. 4. RIA of 1310 nm light by various fibers irradiated from a ^{60}Co gamma source at comparably low dose rates. The data can be fitted with the Power Law (1).

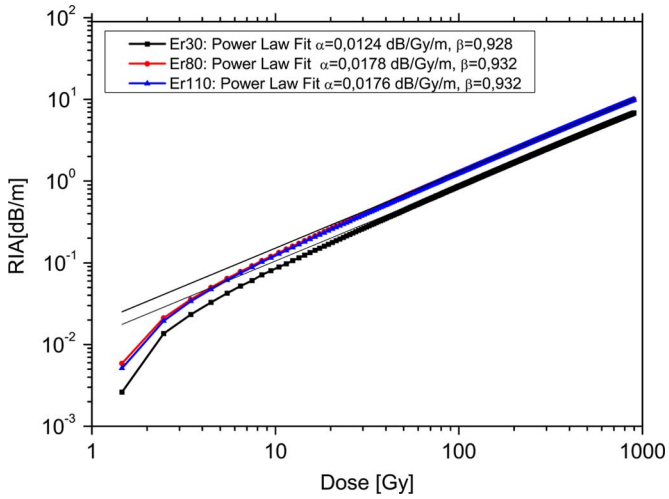

Fig. 5. RIA of 1310 nm light in Er doped fibers irradiated from a ^{60}Co gamma source. For significantly different dopant concentrations RIA behavior appears quite comparable. The data has been fitted according to the Power Law (1).

regime may take up to 1 hour and requires receiving roughly 10 Gy. This is indicative for an improved radiation hardness at lower dose rates, in accordance with (3). Moreover, before RIA totally darkens the fiber, higher resistivity against irradiation damage can be observed. This regime of higher radiation hardness starts at about 10000 Gy. Nevertheless, in a large intermediate range between 10 and 10000 Gy the Power Law describes the RIA extremely well for all projectiles. This is an advantage because it allows us to compare the radiation hardness of various fibers directly by just extracting two coefficients of the Power Law from the data.

A. *Irradiation With Gamma-Rays*

With respect to gamma irradiation we have investigated dose rates differing vastly in magnitude. For higher dose rates of 0.21 Gy/s it is observed that optical fibers are irrecoverably destroyed within one hour. Moreover, we find that during the first 10 minutes the RIA increases approximately quadratically, possibly due to a charge build-up in the fiber core, irradiative heating, or radiation induced change of the dispersion. At such high dose rates the RIA can not be satisfactorily fit by the Power Law and a multi-exponential fit has to be used instead (4). At 10 times lower dose rates of about 0.01 Gy/s the RIA is much more moderate and the effects become quite comparable to previous studies [19]. The transmission loss remains significant after 1000 Gy and the RIA for Er doped fibers is $\alpha_\gamma = 0.0178(4)$ dB·m^{-1}Gy^{-1} (see Figs. 4 and 5). This result exactly follows the (1) with an exponent $\beta_\gamma = 0.93$. A direct comparison between SMF28 (Corning), Yb1200 (Liekki), and Er80 (Liekki) is made in Fig. 4. The most sensitive fibers are Er doped and degrade about 2.6 times faster than Yb1200, and about 80 times faster than SMF28. The Er dopant concentration itself, however, appears to play only a minor role for the RIA, as can be seen from Fig. 5. Within the measurement accuracy the Er110 and Er80 degraded in exactly the same way ($\alpha \approx 0,0177$ dB·m^{-1}Gy^{-1}), and only Er30 was slightly less sensitive ($\alpha = 0.0124$ dB·m^{-1}Gy^{-1}). In other words, an increase in the dopant concentration by a factor 3.7 increases the radiation sensitivity by only 1.44. Such a small increase is inconsistent with the general trend in Fig. 1 that the sensitivity scales with $C^{1.37}$. Therefore we can assume that the general trend in Fig. 1 is caused by the concentration or variation of the various codopants used by different producers.

B. *Irradiation With Protons*

After irradiation with 180 MeV protons in some fibers the final transmission became nearly negligible. Erbium doped fibers lost up to 98% of their transmission, and even SMF28 lost a few percent. Such highly energetic protons can not be shielded efficiently in space. Based on SRIM simulations [37] it becomes clear that the effective energy loss per proton is rather small, reaching ≈0.09 eV/Å, which corresponds to 5.85 keV energy deposition per proton in the fiber core. At a particle flux of $9 \cdot 10^9$ cm^{-2}s^{-1} the dose rate in the core would then be approximately 7.1 Gy/s. Comparison with the stopping power for SiO_2 of $S_{180\,\mathrm{MeV}} = 4$ MeVcm^{2}gm^{-1} given by NIST-PSTAR provides a similar value: 7.26 Gy/s. At such dose rates the RIA by 180 MeV protons can be fitted over a large range by the Power Law (1), leading to the coefficients $\alpha_{180\,\mathrm{MeV}} = 0.022(1)$ dB·m^{-1}Gy^{-1} and $\beta_{180\,\mathrm{MeV}} = 0.91$. Thus, the RIA is found to be very comparable to gamma irradiation at 1.17 MeV. With regard to possible nuclear fission events that could be initiated at these projectile energies we estimate that they would have a probability of <2% in SiO_2. Inspection of the data does not indicate that nuclear reactions have caused any significant deviation from the Power Law.

Upon irradiation with 20 MeV protons, the transmission of SMF28 did not decrease significantly, while Er and Yb doped fibers showed measurable effects. Erbium fibers appeared by about a factor 2 more sensitive than ytterbium doped ones, with a total transmission loss of 35% after 8000 s of irradiation (dose $\sim 8 \cdot 10^5$ Gy). The ytterbium doped fiber lost approximately 15% of transmission under similar conditions and duration. TRIM simulations for 20 MeV protons in SiO_2 suggest an energy deposition of 0.5 eV/Å, corresponding to an energy loss of 32.6 keV per proton, while passing through the core. Thus,

at a particle flux of $2.8 \cdot 10^{10}$ cm^{-2}s^{-1} the core receives a dose rate of 124 Gy/s. This value compares well to a dose rate of 103 Gy/s that is calculated when using the tabulated stopping power for SiO_2 ($S_{20\,\mathrm{MeV}} = 21$ MeVcm^{2}gm^{-1}) provided by NIST-PSTAR. An attenuation coefficient of $\alpha_{20\,\mathrm{MeV}} = 0.02$ dB·m^{-1}Gy^{-1} is observed in the region from 1 to 3 kGy. This is quite close to losses induced by gamma radiation. Due to the high flux it is, however, not possible to fit the data over a more extended dose range. Especially at higher total dose $\beta_{20\,\mathrm{MeV}}$ appears to become significantly smaller than 1, which indicates a saturation effect.

C. Irradiation With Neutrons

Fibers that have been irradiated with neutrons having 20 MeV and 180 MeV have been found to degrade only weakly. In most cases simply no effect could be experimentally observed. Nevertheless, in the case of Er doped fibers, the RIA showed some shallow exponential increase of less than 1% in 4 hours, when a flux of $\approx 3 \cdot 10^4$ cm^{-2}s^{-1} was applied. Although quite small, there is resemblance to the other types of radiation. Due to the weakness of the experimental signal it is yet impossible to quantify such RIA caused by neutrons. However, it should be taken into account that the flux applied here has been comparably small and that neutrons naturally have fewer interactions with the matrix. Recently the TSL has been upgraded and much higher neutron fluxes can now be achieved, which opens up interesting opportunities for improved experiments regarding the subject.

D. Recovery and Annealing

In most cases, at least part of the transmission of the irradiated fibers recovers after the radiation exposure has ceased. When Er80 is irradiated with 180 MeV protons, the fiber rapidly becomes completely dark, but at room temperature it recovers about 0.1% of its transmission within 13 hrs, which is a small but significant amount. After irradiation with 20 MeV protons, the Er80 fiber recovers 1.2%/hr, and the Yb1200 fiber even faster. In general, however, we find that the transmission $T(t)$ does not recover at a constant rate, which is pointing towards some annealing reaction kinetics of higher order. When heating the fiber with increasing temperature, we observe that the recovery depends significantly on such annealing. After heating to 450 K, the Er80 recovered to 70% of its original transmission. A typical annealing curve comparing Er80, Yb1200 and SMF28 fibers is shown in Fig. 6. It demonstrates that annealing of the Er doped fiber is most efficient. Annealing at 450 K is found to recover several dB/m within one day. The time dependence of the transmission recovery can be perfectly modeled by first order kinetics.

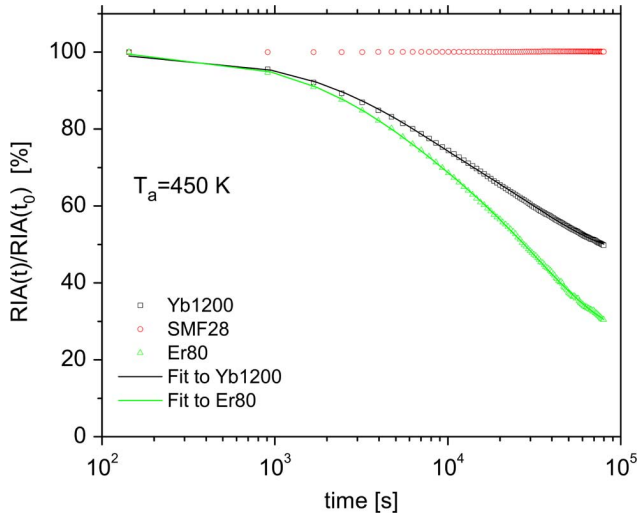

Fig. 6. Annealing of doped irradiated fibers at 450 K leads to a significant recovery of the transmission when compared to the undoped SMF28 fiber. This data has been fit using a sum of two decay reactions in each fiber using (5), corresponding to two types of color centers with slightly different binding energy. In the present experimental configuration no change of the RIA was observable for the single mode fiber SMF28.

IV. Discussion

From our experiments we conclude that RIA does not significantly depend on the type of radiation, even if the underlying energy absorption mechanism varies for different types of projectiles. While gamma energy is efficiently converted to electron energy, protons are continuously decelerated and lose energy over a much longer geometrical range. Proton impact leads to damage traces similar to fission tracks in the solid matrix. Compared to this, neutrons interact only with the nuclei, leading to nuclear activation. Neutron-induced nuclear reactions can instantly deposit a large amount of energy within a small volume. The three types of projectiles studied here are absorbed with largely different cross sections in the matrix material. The total received dose can be easily calculated from the tabulated mass attenuation coefficients S (NIST, PSTAR) for protons or using the Monte-Carlo trajectory simulation package TRIM/SRIM [37]. Similarly, gamma ray attenuation can be calculated from tabulated data at NIST, using the program XCOM.

The dose rate received when subjecting a material of thickness dx, density ρ, and exposed surface dA with particles of flux N is given by $D = NdA \cdot S\rho dx$. For gamma irradiation we do not rescale dose rates to quartz, but use the dose calibrated for ambient air. This is justified to keep our values comparable to the works tabulated in Table I. For protons we calculate the dose based on TRIM calculations, because the particle energy may change slightly while passing through cladding and core. From such simulations we estimate dose rates of $1.24 \cdot 10^2$ Gys^{-1}, and $7.1 \cdot 10^{-1}$ Gys^{-1} for 20, and 180 MeV, respectively. Such dose rates are considerably higher than typically found in space. Moreover, this means that protons deposit up to 10^6 times more energy per gram into the material. Neutron energy dose rates from interaction between the magnetic moment of the neutron and the electrons can be estimated according to [38]:

$$-dE/\rho ds = 5 \cdot 10^{-9} \left(\gamma_r^2 - 1\right) \left(\gamma_r^2 + 3\right) [\mathrm{MeV\ cm^2/g}] \quad (2)$$

where $\gamma_r = \sqrt{1 - v^2/c^2}$ is the relativistic dilation for neutrons having the velocity v. For 20 and 180 MeV neutrons the attenuation is then $8.7 \cdot 10^{-10}$ [MeV cm^2/g] and $9.27 \cdot 10^{-9}$ [MeV cm^2/g], respectively. From this estimate we obtain dose rates that are about 10 orders of magnitude less than for protons. However, the ionization caused by magnetic interaction

described by (2) is negligibly weak compared to the various nuclear reactions caused by neutrons: (n, p), (n,γ), (n,α) and (n, Xn). For such reactions energy deposition is not quasi-continuous and therefore the concept of a stopping power fails. As these interactions are about a million times stronger with typical cross sections of a few barn they dominate the effects. Nevertheless, at least at the flux applied here the damage observed was quite moderate and for space applications the RIA caused by neutrons can presumably be neglected.

Little is presently known about dose rate effects of RIA, and inspection of the fiber database for some selected fibers does not lead to the observation of clear trends. Most studies used low dose rates, which are still much higher than in space. A related study by Williams and coworkers [25] suggests a modified Power Law like

$$A(D) = \alpha_0 R^{1-\beta} D^{\beta} \tag{3}$$

With R the dose rate and α_0 a reduced pre-exponential factor. Williams, however, observed experimentally that the exponent of R appears to be even smaller than theory predicts. Consequently, at low dose rates the measurement ambiguity caused by variations in e.g., the individual fiber composition, calibration procedure or other errors presumably exceeds such dose rate effects significantly. In general, because natural dose rates in space are significantly lower, RIA will be significantly decreased.

Moreover, it is important to understand that accurate modeling of RIA with only two parameters obviously has its limits. From our studies and comparison of the literature we conclude that RIA after receiving the dose $D(t)$ can be approximated by two complementary approaches. For simple cases, e.g., for fibers that are comparably hard to radiation, the *exponential Power Law* (1) is found to correspond to many data. (1) has the advantage, that only two parameters have to be determined for an accurate long term prediction of the fiber condition in space. This makes (1) a preferred choice for predictive modeling of space missions. However, in some cases, especially under intense irradiation, the Power Law fails and can not fit the data accurately enough. Under such circumstances the *saturating exponentials model* [39]

$$A(D) = \sum_i a_i(1 - \exp(-D/\tau_i)) \tag{4}$$

represents the experimental observation much better and appears also to be closer to the underlying physics. Each term in (4) represents a type of an absorbing defect. In general we find that for rare earth doped fibers (4) is probably more appropriate and can fit the data in Fig. 3 more accurately in the very low or very high dose regime, because more fit parameters can be introduced. But (1) appears to be sufficiently accurate to provide a trustable *upper limit* for *long-term* RIA. Fitting of the experimental data shown in Fig. 3 with (4) based on two defect types or color centers $(i = 1, 2)$ leads to a significantly smaller residuum compared to the Power Law fit.

Radiation induced color centers arise, when electron-hole pairs find no possibility to recombine in the solid matrix, and they are often represented by weakly bound (solvated or trapped) electrons. The concentration C_i of color centers in the matrix can be modeled from first order chemical kinetics

$$dC_i/dt = -k_i C_i \tag{5}$$

The back reaction rates $k_i = k_{i0} \exp(-\varepsilon_i/k_b T)$ relate the energy barrier ε_i of the color center of type i to the phonon energy $k_b T$, where k_b is the Boltzmann-constant and T is the temperature. Such recombination rates can be derived from $C_i = C_{i,t=0} \exp(-k_i t)$ using an Arrhenius plot (e.g., plotting $\ln(k)$ versus $1/T$), providing activation energies ε_i and pre-exponential factor k_{i0}. For the two fibers that we have investigated here, we find that the weakest color center binding energy ε_i is about 20 meV for ER80-4/125 and 40 meV for Yb1200-4/125-DC. In our analysis we do not consider any higher order reaction kinetics, which would not be justified for this type of process. Our experimental data in Fig. 6 can be fitted very well using two types of color centers in each fiber, a weakly bound one and a slightly stronger bound one.

From a general perspective, it is possible to interpret RIA as a reaction with irradiation being a reactive component causing the forward reaction towards color center generation, while phonons or heat and visible photons will drive the reaction equilibrium towards the backward recombination reaction:

$$[\mathrm{Bulk}] + [\mathrm{RE}] \underset{T,h\nu}{\overset{n,p,\gamma}{\rightleftharpoons}} [\mathrm{Bulk}] + [\mathrm{RE}] + [\mathrm{CC}] \tag{6}$$

In principle, this can be treated with a semi-empirical radio-chemistry model. Only a few dominating reaction rates, in the present case two, are needed to model the decay of RIA with minor deviation from the experimental observation. The resulting overall reaction behavior will always be dominated by a limited number of activation barriers, regardless of their physical or chemical origin. The associated reactions can be of primary, secondary, or consecutive nature. Even matrix and point defect interactions could, in principle, be modeled by such a multiple reaction rate model. Consequently, for a constant dose the RIA should always saturate, which is presently not correctly described by the power law. Such a saturation of the RIA can for example be observed in the case of proton irradiation in Fig. 3. With respect to long-term space applications, it will be crucial to achieve a backward reaction rate which is within the same order of magnitude or even higher than the irradiation driven forward reaction rate.

The observable partial instability of RIA opens up interesting possibilities to improve the radiation hardness of rare earth doped fibers. Preferred approaches appear to be either heating or irradiation with visible or infrared light. In this context it should be once more stressed that pump laser light can improve the radiation hardness significantly [27] and that presumably already little amounts of suitable energy coupled into the core could be sufficient to extend fiber survival times significantly. In the present work we have not reported on the influence of active lasing to RIA. The reason is, that active lasing itself sometimes leads to the generation of color centers, and consequently the situation can easily become quite complex. Moreover, the generation of color centers has been observed to

be different for cw-lasing and for pulsed lasing. In this respect, RIA of optically pumped fibers will be an interesting subject of future studies.

V. Conclusion

Radiation induced absorption in rare earth doped fibers has been investigated. A detailed comparison based on a database containing about 60 RIA measurements by different authors leads to the conclusion that the rare-earth dopant concentrations are not primarily responsible for radiation sensitivity. Instead, co-dopants appear to be the major reason for radiation sensitivity. This is experimentally confirmed for the case of Er-doped fibers. Moreover, we find that radiation induced absorption is only dose dependent, it does not depend on the type and energy of the projectile. RIA shows all typical signatures for the generation of weakly bound color centers. We demonstrate that RIA can be at least partially annealed at quite moderate temperatures around 450 K. We suggest that the instability of radiation induced color centers, in particular in the case of Er-doped fibers, represents a major key for the development of fiber components and lasers for space missions.

Acknowledgment

The authors enjoyed helpful discussions with T. Udem and H. Schröder on the subject.

References

[1] M. J. F. Digonnet, *Rare Earth Doped Fiber Lasers and Amplifiers*, 2nd ed. New York: Marcel Dekker, 2001.

[2] T. Eidam, S. Hanf, E. Seise, T. V. Andersen, T. Gabler, C. Wirth, T. Schreiber, J. Limpert, and A. Tunnermann, "Femtosecond fiber cpa system emitting 830 w average output power," *Opt. Lett.*, vol. 35, no. 2, pp. 94–96, 2010.

[3] K. Tamura, E. P. Ippen, H. A. Haus, and L. E. Nelson, "77-fs pulse generation from a stretched-pulse mode-locked all-fiber ring laser," *Opt. Lett.*, vol. 18, no. 13, pp. 1080–1082, 1993.

[4] G. Krauss, S. Lohss, T. Hanke, A. Sell, S. Eggert, R. Huber, and A. Leitenstorfer, "Synthesis of a single cycle of light with compact erbium-doped fibre technology," *Nature Photon.*, vol. 4, no. 1, pp. 33–36, 2009.

[5] P. Kubina, P. Adel, F. Adler, G. Grosche, T. W. Hänsch, R. Holzwarth, A. Leitenstorfer, B. Lipphardt, and H. Schnatz, "Long term comparison of two fiber based frequency comb systems," *Opt. Expr.*, vol. 13, no. 3, pp. 904–909, 2005.

[6] *PSS-01-609 Radiation Design Handbook,* 1st ed., ESA, 1993.

[7] NASA Electronic Parts and Packaging (NEPP) Program [Online]. Available: http://nepp.nasa.gov

[8] European Space Components Information Exchange System [Online]. Available: https://escies.org

[9] M. N. Ott, "Radiation effects data on commercially available optical fiber: Database summary," in *Proc. IEEE Radiation Effects Data Workshop, Conjunction With IEEE Nuclear and Space Radiation Effects Conf.*, S. C. Witczak, Ed., New York, 2002, vol. 49, no. 9, pp. 24–31, IEEE, 10017.

[10] E. J. Friebele, M. E. Gingerich, and G. H. Sigel, "Effect of ionizing-radiation on optical attenuation in doped silica and plastic fiberoptic waveguides," *Appl. Phys. Lett.*, vol. 32, no. 10, pp. 619–621, 1978.

[11] G. M. Williams, M. A. Putnam, C. G. Askins, M. E. Gingerich, and E. J. Friebele, "Radiation effects in erbium-doped optical fibers," *Electron. Lett.*, vol. 28, no. 19, pp. 1816–1818, 1992.

[12] G. M. Williams, M. A. Putnam, C. G. Askins, M. E. Gingerich, and E. J. Friebele, "Radiation-induced coloring of erbium-doped optical fibers," *Proc. SPIE, Optical Materials Reliability and Testing: Benign and Adverse Environments*, vol. 1791, pp. 274–283, 1993.

[13] D. L. Griscom, M. E. Gingerich, and E. J. Friebele, "Radiation-induced defects in glasses—Origin of power-law dependence of concentration on dose," *Phys. Rev. Lett.*, vol. 71, no. 7, pp. 1019–1022, 1993.

[14] G. M. Williams, M. A. Putnam, and E. J. Friebele, "Space radiation effects on erbium doped fibers," *Proc. SPIE, Photonics for Space Environments IV*, vol. 2811, pp. 30–37, 1996.

[15] M. Alam, J. Abramczyk, J. Farroni, U. Manyam, and D. Guertin, "Passive and active optical fibers for space and terrestrial applications," *Proc. SPIE, Photonics for Space Environments XI*, vol. 6308, pp. U86–U99, 2006.

[16] O. Berne, M. Caussanel, and O. Gilard, "A model for the prediction of edfa gain in a space radiation environment," *IEEE Photon.s Technol. Lett.*, vol. 16, no. 10, pp. 2227–2229, 2004.

[17] H. Henschel, O. Kohn, H. U. Schmidt, J. Kirchhof, and S. Unger, "Radiation-induced loss of rare earth doped silica fibres," *IEEE Trans. Nucl. Sci.*, vol. 45, no. 3, pp. 1552–1557, Jun. 1998.

[18] S. Girard, B. Tortech, E. Regnier, M. Van Uffelen, A. Gusarov, Y. Ouerdane, J. Baggio, P. Paillet, V. Ferlet-Cavrois, A. Boukenter, J. P. Meunier, F. Berghmans, J. R. Schwank, M. R. Shaneyfelt, J. A. Felix, E. W. Blackmore, and H. Thienpont, "Proton- and gamma-induced effects on erbium-doped optical fibers," *IEEE Trans. Nucl. Sci.*, vol. 54, no. 6, pp. 2426–2434, Dec. 2007.

[19] B. P. Fox, K. Simmons-Potter, J. H. Simmons, W. J. Thomes, R. P. Bambha, and D. A. V. Kliner, "Radiation damage effects in doped fiber materials," *Proc. SPIE, Fiber Lasers V: Technology, Systems, and Applications*, vol. 6873, pp. U277–U285, 2008.

[20] B. P. Fox, K. Simmons-Potter, W. J. Thomes, and D. A. V. Kliner, "Gamma-radiation-induced photodarkening in unpumped optical fibers doped with rare-earth constituents," *IEEE Trans. Nucl. Sci.*, vol. 57, no. 3, pp. 1618–1625, Jun. 2010.

[21] B. P. Fox, Z. V. Schneider, K. Simmons-Potter, W. J. Thomes, D. C. Meister, R. P. Bambha, and D. A. V. Kliner, "Spectrally resolved transmission loss in gamma irradiated yb-doped optical fibers," *IEEE J. Quantum Electron.*, vol. 44, no. 5–6, pp. 581–586, 2008.

[22] T. S. Rose, D. Gunn, and G. C. Valley, "Gamma and proton radiation effects in erbium-doped fiber amplifiers: Active and passive measurements," *J. Lightw. Technol.*, vol. 19, no. 12, pp. 1918–1923, 2001.

[23] H. Henschel, O. Kohn, W. Lennartz, S. Metzger, H. U. Schmidt, J. Rosenkranz, B. Glessner, and B. R. L. Siebert, "Comparison between fast neutron and gamma irradiation of optical fibres," *IEEE Trans. Nucl. Sci.*, vol. 45, no. 3, pp. 1543–1551, Jun. 1998.

[24] H. Henschel and O. Kohn, "Regeneration of irradiated optical fibres by photobleaching?," *IEEE Trans. Nucl. Sci.*, vol. 47, no. 3, pp. 699–704, Jun. 2000.

[25] G. M. Williams, B. M. Wright, W. D. Mack, and E. J. Friebele, "Projecting the performance of erbium-doped fiber devices in a space radiation environment," *Proc. SPIE, Optical Fiber Reliability and Testing*, vol. 3848, pp. 271–280, 1999.

[26] F. Mady, M. Benabdesselam, and W. Blanc, "Thermoluminescence characterization of traps involved in the photodarkening of ytterbium-doped silica fibers," *Opt. Lett.*, vol. 35, no. 21, pp. 3541–3543, 2010.

[27] E. W. Taylor and J. Liu, E. W. Taylor, Ed., "Ytterbium-doped fiber laser behavior in a gamma-ray environment," *Proc. SPIE, Photonics for Space Environments X*, vol. 5897, 2005.

[28] S. Girard, Y. Ouerdane, B. Tortech, C. Marcandella, T. Robin, B. Cadier, J. Baggio, P. Paillet, V. Ferlet-Cavrois, A. Boukenter, J. P. Meunier, J. R. Schwank, M. R. Shaneyfelt, P. E. Dodd, and E. W. Blackmore, "Radiation effects on ytterbium- and ytterbium/erbium-doped double-clad optical fibers," *IEEE Trans. Nucl. Sci.*, vol. 56, no. 6, pp. 3293–3299, Dec. 2009.

[29] H. Henschel, O. Kohn, and U. Weinand, "Radiation hardening of pure silica optical fibres by high pressure hydrogen treatment," in *Proc. 6th Euro. Conf. Radiation and Its Effects on Components and Systems*, 2002, pp. 141–149.

[30] K. V. Zotov, M. E. Likhachev, A. L. Tomashuk, M. M. Bubnov, M. V. Yashkov, and A. N. Guryanov, "Radiation-resistant erbium-doped silica fibre," *Quantum Electron.*, vol. 37, no. 10, pp. 946–949, 2007.

[31] K. V. Zotov, M. E. Likhachev, A. L. Tomashuk, M. M. Bubnov, M. V. Yashkov, A. N. Guryanov, and S. N. Klyamkin, "Radiation-resistant erbium-doped fiber for spacecraft applications," *IEEE Trans. Nucl. Sci.*, vol. 55, no. 4, pp. 2213–2215, Aug. 2008.

[32] E. J. Friebele, "Radiation protection of fiber optic materials—Effect of cerium doping on radiation-induced absorption," *Appl. Phys. Lett.*, vol. 27, no. 4, pp. 210–212, 1975.

[33] S. Girard, A. Laurent, M. Vivona, C. Marcandella, T. Robin, B. Cadier, A. Boukenter, and Y. Ouerdane, "Radiation effects on fiber amplifiers: Design of radiation tolerant yb/er-based devices," *Proc. SPIE, Fiber Lasers VIII: Technology, Systems, and Applications*, vol. 7914, p. 79142, 2001.

[34] P. Jelger, M. Engholm, L. Norin, and F. Laurell, "Degradation-resistant lasing at 980 nm in a yb/ce/al-doped silica fiber," *J. Opt. Soc. Amer. B, Opt. Phys.*, vol. 27, no. 2, pp. 338–342, 2010.

[35] S. Holm, A. Johansson, S. Kullander, and D. Reistad, "New accelerators in uppsala," *Physica Scripta*, vol. 34, no. 6A, p. 513, 1986.
[36] A. Prokofiev, J. Blomgren, O. Byström, C. Ekström, S. Pomp, U. Tippawan, V. Ziemann, and M. Österlund, "The tsl neutron beam facility," in *Proc. 10th Symp. Neutron Dosimetry*, J. MacDonald, Ed., Uppsla, Sweden, 2007, vol. 126, pp. 18–22, ser. Rad. Prot. Dos., Oxford Univ. Press.
[37] J. F. Ziegler, J. P. Biersack, and M. D. Ziegler, SRIM the Stopping and Range of Ions in Matter, 2009 [Online]. Available: http://www.srim.org
[38] R. Vora, V. N. Neelavathi, J. E. Turner, T. S. Subramanian, and M. A. Prasad, "Semiclassical estimation of neutron stopping power," *Phys. Rev. B*, vol. 3, no. 9, p. 2929, 1971.
[39] Y. Morita and W. Kawakami, "Dose-rate effect on radiation-induced attenuation of pure silica core optical fibers," *IEEE Trans. Nucl. Sci.*, vol. 36, no. 1, pp. 584–590, Feb. 1989.
[40] M. Alam, J. Baramczyk, U. Manyam, J. Farroni, and D. Guertin, Performance of Optical Fibers in Space Radiation Environments, Jun. 27, 2006 [Online]. Available: http://www.nufern.com/whitepapers.php